Molecular Vision 2013; 19:2135-2150 <http://www.molvis.org/molvis/v19/2135>
Received 30 May 2013 | Accepted 29 October 2013 | Published 1 November 2013

An ophthalmic solution of a peroxisome proliferator-activated receptor gamma agonist prevents corneal inflammation in a rat alkali burn model

Masaaki Uchiyama,[1,2] Akira Shimizu,[2] Yukinari Masuda,[2] Shinya Nagasaka,[2] Yuh Fukuda,[2] Hiroshi Takahashi[1]

[1]Department of Ophthalmology, Nippon Medical School, Tokyo, Japan; [2]Department of Analytic Human Pathology, Nippon Medical School, Tokyo, Japan

Purpose: We clarified the effects of an ophthalmic solution of a peroxisome proliferator-activated receptor gamma (PPARγ) agonist on corneal inflammation and wound healing after alkali burn injury in rats.
Methods: After alkali exposure, either an ophthalmic solution with 0.1% pioglitazone hydrochloride (the PPARγ group) or vehicle (the vehicle group) was topically applied to the cornea until day 14. Histological, immunohistochemical, and real-time reverse transcription polymerase chain reaction analysis were performed.
Results: After alkali injury, PPARγ expression increased, with the infiltration of many inflammatory cells. The infiltration of neutrophils and macrophages started from the corneal limbus within 6 h, and developed in the corneal center by day 7, with associated neovascularization. The accumulation of α-smooth muscle actin-positive myofibroblasts and the deposition of type III collagen were noted on day 14. The histological changes were suppressed significantly by treatment with the ophthalmic solution of the PPARγ agonist. In addition, the number of infiltrating M2 macrophages in the cornea was increased by PPARγ agonist treatment. In real-time reverse transcription polymerase chain reaction analysis, the messenger ribonucleic acid expression levels of interleukin-1β (IL-1β), IL-6, IL-8, monocyte chemoattractant protein-1, tumor necrosis factor-α, transforming growth factor beta 1, and vascular endothelial growth factor-A were decreased in the PPARγ group compared to the vehicle group in the early periods of corneal inflammation.
Conclusions: The ophthalmic solution of the PPARγ agonist inhibited inflammation, decreased the fibrotic reaction, and prevented neovascularization in the cornea from the early phase after alkali burn injury. The ophthalmic solution of the PPARγ agonist may provide a new treatment strategy with useful clinical applications for corneal inflammation and wound healing.

Peroxisome proliferator-activated receptors (PPARs) are ligand-activated transcription factors in the nuclear hormone receptor superfamily related to retinoid, steroid, and thyroid hormone receptors [1,2]. The PPARs family is represented by three members: PPARα, PPARβ/δ, and PPARγ [3]. PPARγ, a key transcription factor involved in adipocyte differentiation, lipid, and glucose homeostasis, is an important therapeutic target for type 2 diabetes and metabolic syndrome [4]. Apart from a role in the transcriptional regulation of metabolism, PPARγ also suppresses the expression of several genes involved in inflammation, independent of the receptor's DNA binding [1,5]. PPARγ exerts anti-inflammatory effects by negatively regulating the expression of proinflammatory genes induced in response to macrophage differentiation and activation [6,7]. Recent studies have clarified the widespread effects of PPARγ not only in inflammation but also in wound healing [8].

PPARγ ligands possess antiangiogenic properties, and can inhibit the proangiogenic effects of vascular endothelial growth factor (VEGF) and endothelial cell migration [9]. In addition, a PPARγ agonist inhibited fibrotic changes by suppressing transforming growth factor beta (TGF-β) signaling [10]. The anti-inflammatory effects of PPARγ have been observed in various organs, although previous investigations mainly focused on internal organs, such as the kidneys [11], heart [12], and lungs [13]. In the alkali-burned cornea, Saika et al. suggested that introducing the PPARγ gene suppressed macrophage invasion and the generation of myofibroblasts [14].

Several corneal studies on PPARγ using gene transfer [14] or a micropellet technique [15] have been reported. However, no ocular study used an ophthalmic solution of the PPARγ agonist. In the present study, we compounded an ophthalmic solution using pioglitazone hydrochloride, a thiazolidinedione that is a high-affinity ligand for PPARγ.

Correspondence to: Akira Shimizu, Department of Analytic Human Pathology, Nippon Medical School, 1-1-5 Sendagi, Bunkyo-ku, Tokyo 113-8602, Japan; Phone: +81-3-3822-2131; FAX: +81-3-5685-3067; email: ashimizu@nms.ac.jp.

Thiazolidinediones are mainly used as insulin-sensitizing drugs for patients with type 2 diabetes mellitus, but have been shown to have a potential role in attenuating vascular fibrosis and inhibiting inflammatory responses [16,17]. We thus examined the effects of the ophthalmic solution of pioglitazone hydrochloride on corneal inflammation and wound healing using a rat alkali burn model. We focused on the effects on inflammatory cell infiltration, myofibroblast accumulation and the fibrotic reaction, and neovascularization in the alkali-burned cornea.

METHODS

Ophthalmic solution of peroxisome proliferator-activated receptor gamma: In the present study, we compounded two kinds of ophthalmic solutions, a vehicle solution and a 0.1% pioglitazone hydrochloride solution. The ophthalmic vehicle solution was prepared using 100 ml NaCl-based PBS (0.01 M; pH 7.4) which was prepared with disodium hydrogenphosphate 12-water 232 g, sodium dihydrogenphosphate dihydrate 23.7 g, and distilled water 4000 ml and 0.1 ml polyoxyethylene sorbitan monooleate (Wako Pure Chemical Industries, Osaka, Japan). The ophthalmic solution including 0.1% pioglitazone hydrochloride was prepared as 30 ml of the vehicle solution with 30 mg pioglitazone hydrochloride (Molekula Ltd, Dorset, UK). The ophthalmic solutions were kept in the refrigerator at 4 °C, and used within a month of compounding.

Animal model of a corneal alkali burn and treatment with the ophthalmic solutions: Animal experiments were performed in compliance with the experimental animal ethics review committee of Nippon Medical School, Tokyo, Japan, and all procedures conformed to the Association for Research in Vision and Ophthalmology (ARVO) Statement for the Use of Animals in Ophthalmic and Visual Research. Eight-week-old male Wistar rats (Sankyo Laboratory Service, Tokyo, Japan) were used for all experiments in the present study (n=12 per time point).

The corneal alkali burn was made by placing a 3.2 mm in diameter circular piece of filter paper soaked in 1N NaOH on the central cornea for 1 min under general isoflurane anesthesia. Immediately after alkali exposure, the cornea was rinsed with 40 ml physiologic saline. The procedure was performed unilaterally (right eye) in each rat. Then, either an ophthalmic solution of 0.1% pioglitazone hydrochloride (the PPARγ group) or vehicle (the vehicle group) was topically instilled onto the animals' ocular surfaces. In each group, topical administration was continued twice a day until the end point. At 6 h and on day 1, 2, 4, 7, and 14 after the alkali burn, the rats were euthanized by exsanguination under general isoflurane anesthesia. The eyeballs were enucleated for a histological and immunohistochemical analysis and real-time reverse transcription polymerase chain reaction (RT–PCR) after macroscopic examination. The contralateral eyes (left eyes) were used as uninjured controls (normal). For the real-time RT–PCR analyses, the corneal tissues were immediately put into RNAlater solution (Life Technologies, Carlsbad, CA) and stored at −80 °C.

Histological and immunohistochemical analysis: The eyeballs were fixed in 10% buffered formalin and embedded in paraffin for a light microscopic analysis. Tissues were stained with hematoxylin and eosin (H&E) for the histopathological examination. Naphthol AS-D chloroacetate esterase staining was performed to detect infiltrating neutrophils [18].

The following primary antibodies were used for the immunohistochemical analysis: 1) monoclonal mouse antirat ED1 antibody (BMA, Nagoya, Japan) to detect the infiltrating macrophages; 2) monoclonal mouse antirat ED2 antibody (BMA) to detect M2 macrophages, because rat ED2 is also called CD163, which is expressed on M2 macrophages; and 3) monoclonal mouse antirat ED3 antibody (BMA) to detect activated macrophages. Although rat ED3 is a marker for tissue-fixed macrophages, bone marrow–derived macrophages stimulated by T cells are also positive for ED3, indicating that the antirat ED3 antibody can detect activated macrophages [19]. Additional antibodies were also used, including 4) polyclonal rabbit antirat thrombomodulin (TM) antibody (courtesy of Dr. David Stern, Columbia University, New York, NY) to detect neovascular endothelial cells [20,21]; 5) polyclonal goat antitype I collagen (Southern Biotech, Birmingham, AL), 6) polyclonal goat antitype III collagen (Southern Biotech) to detect collagens [22]; 7) monoclonal mouse anti-α-smooth muscle actin (α-SMA; Dako, Glostrup, Denmark) to detect myofibroblasts [23]; and 8) monoclonal mouse antirat PPARγ antibody (E-8: Santa Cruz Biotechnology, Santa Cruz, CA) to detect PPARγ-expressing cells.

For the immunohistochemical analysis of ED1, ED2, TM, type I and type III collagens, α-SMA, and PPARγ, 10%-buffered, formalin-fixed, paraffin-embedded tissue sections were used. The specimens were stained with the standard avidin-biotin-peroxidase complex technique. The percentage of the positive pixel intensity of type III collagen and the α-SMA-positive cells in 200X corneal regions on day 14 was analyzed quantitatively using a computer-assisted image analysis system and a color image-analyzing software (WinROOF; Mitani, Tokyo, Japan). To detect the ED2- or ED3-positive macrophages, double immunofluorescence staining for ED2 (mouse IgG_1; Texas red) or ED3 (mouse IgG_{2a}; fluorescein isothiocyanate) was performed with frozen

tissue sections. The nuclei counterstaining was performed with 4'-6-diamidino-2-phenylindole (Vectashield, Vector Laboratories, Burlingame, CA).

Real-time reverse transcription–polymerase chain reaction: To examine the mRNA expression levels of interleukin-1β (IL-1β), IL-6, IL-8 (CXCL8), monocyte chemoattractant protein-1 (MCP-1/CCL2), tumor necrosis factor alpha (TNF-α), TGF-β1, and VEGF-A, we used a real-time RT–PCR technique (n=6 per time point). The corneal total RNA was extracted using the Qiagen RNeasy Mini kit (Qiagen, Hilden, Germany) according to the manufacturer's protocol. RNA concentration and purity (A_{260}/A_{280}) were measured using a NanoDrop ND-1000 V 3.2.1 Spectrophotometer (NanoDrop Technologies, Wilmington, DE). The purified total RNA were 1.9–2.2 of A_{260}/A_{280}. cDNA libraries were created with a High Capacity cDNA Reverse Transcription kit (Applied Biosystems, Foster City, CA) according to the manufacturer's protocol from 4 μg total RNA. The gene expression levels were analyzed using 0.3 μl cDNA with real-time quantitative RT–PCR using the THUNDERBIRD SYBR qPCR Mix (TOYOBO, Osaka, Japan) based on real-time detection of accumulated fluorescence according to the manual supplied by the manufacturer (ABI PRISM 7900HT, Applied Biosystems). The normalized value for mRNA expression in each sample was calculated as the relative quantity of relevant primers divided by the relative quantity of the housekeeping gene, β-actin. The sequences of the real-time RT–PCR primers used in this study are listed in Table 1. Quantification was performed using the SDS 2.3 software program (Applied Biosystems).

Statistical analyses: The results are expressed as means±standard error. Differences were evaluated with the Student *t* test using an analytical software program (Excel, Microsoft, Redmond, WA).

RESULTS

Peroxisome proliferator-activated receptor gamma expression in rat corneas: In the normal rat cornea, PPARγ-positive cells were observed in the epithelial basement cells (Figure 1A). In the alkali-burned corneas, PPARγ was mainly expressed on infiltrating neutrophils and macrophages (Figure 1B–D).

The wound healing process after alkali exposure: In the PPARγ and vehicle groups, several types of infiltrating inflammatory cells, including neutrophils and macrophages, were present in the corneal limbus by 6 h after the alkali burn (Figure 2A,E). In the center of the cornea at 6 h after the injury, the corneal epithelium was exfoliated from the stroma, and loose and vacuolar degeneration of the stroma was noted, with the disappearance of the nuclei of the epithelial cells in the alkali-burned cornea (Figure 2I,M). By day 2, the corneal epithelium was regenerated without conjunctivalization, and the surface of the cornea was completely covered. By day 7, the stromal vacuolar degeneration had decreased, and the infiltration of inflammatory cells had increased in the corneal limbus. They also moved to the center of the cornea. Along with inflammatory cell infiltration, neovascularization was noted from the corneal limbus (Figure 2C,G) and progressed to the center of the cornea by day 14 (Figure 2L,P). The development of inflammatory cell infiltration and neovascularization in the PPARγ group occurred later and to a lesser degree compared to the vehicle group on day 14.

Infiltration of neutrophils and macrophages: In the PPARγ and vehicle groups, naphthol AS-D chloroacetate esterase-positive neutrophils and ED1-positive macrophages were noted in the corneal limbus at 6 h after injury, and increased by day 1 after the alkali burn (Figure 3A,B; Figure 4A,B). On day 1, the number of neutrophils (PPARγ group: 41.6±4.0 cells/400X high-power field [HPF]; vehicle group: 57.1±7.0

Table 1. Primer sequences used for the rats gene expression analysis.

Gene	Forward primer sequence (5′-3′)	Reverse primer sequence (5′-3′)
IL-1β	TACCTATGTCTTGCCCGTGGAG	ATCATCCCACGAGTCACAGAGG
IL-6	GTCAACTCCATCTGCCCTTCAG	GGCAGTGGCTGTCAACAACAT
IL-8 (CXCL8)	CCCCCATGGTTCAGAAGATTG	TTGTCAGAAGCCAGCGTTCAC
MCP-1 (CCL2)	AGCCAGATGCAGTTAATGCCC	ACACCTGCTGCTGGTGATTCTC
TNF-α	AAATGGGCTCCCTCTCATCAGTTC	TCTGCTTGGTGGTTTGCTACGAC
TGF-β1	TGGCGTTACCTTGGTAACC	GGTGTTGAGCCCTTTCCAG
VEGF-A	TGTGCGGGCTGCTGCAATGAT	TGTGCTGGCTTTGGTGAGGTTTGA
β-actin	ACCACCATGTACCCAGGCATT	CCACACAGAGTACTTGCGCTCA

IL: interleukin, MCP: monocyte chemoattractant protein, TNF: tumor necrosis factor, TGF: transforming growth factor, VEGF: vascular endothelial growth factor

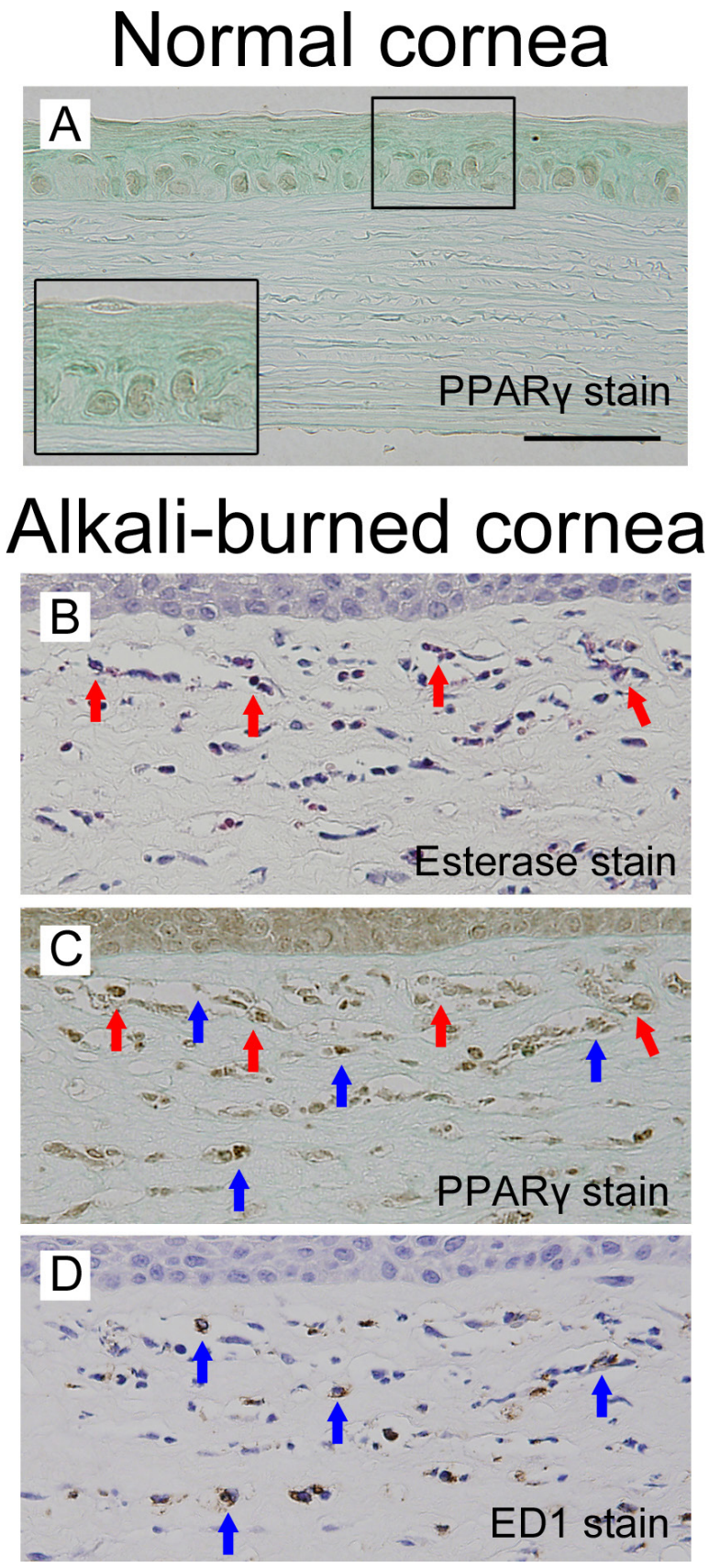

Figure 1. The expression of peroxisome proliferator-activated receptor γ (PPARγ). The expression of PPARγ in the normal cornea (**A**) and in the alkali-burned cornea (**B**–**D**; **A**, **C**: PPARγ stain, **B**: naphthol AS-D chloroacetate esterase stain, **D**: ED1 stain, scale bar: 50 µm). In the normal rat cornea (**A**), PPARγ was expressed mainly on the epithelial basement cells. In the alkali-burned cornea on day 2, serial sections treated with naphthol AS-D chloroacetate esterase (**B**), PPARγ (**C**), and ED1 (**D**) stains showed that PPARγ was expressed on infiltrating naphthol AS-D chloroacetate esterase-positive neutrophils (red arrows) and ED1-positive macrophages (blue arrows).

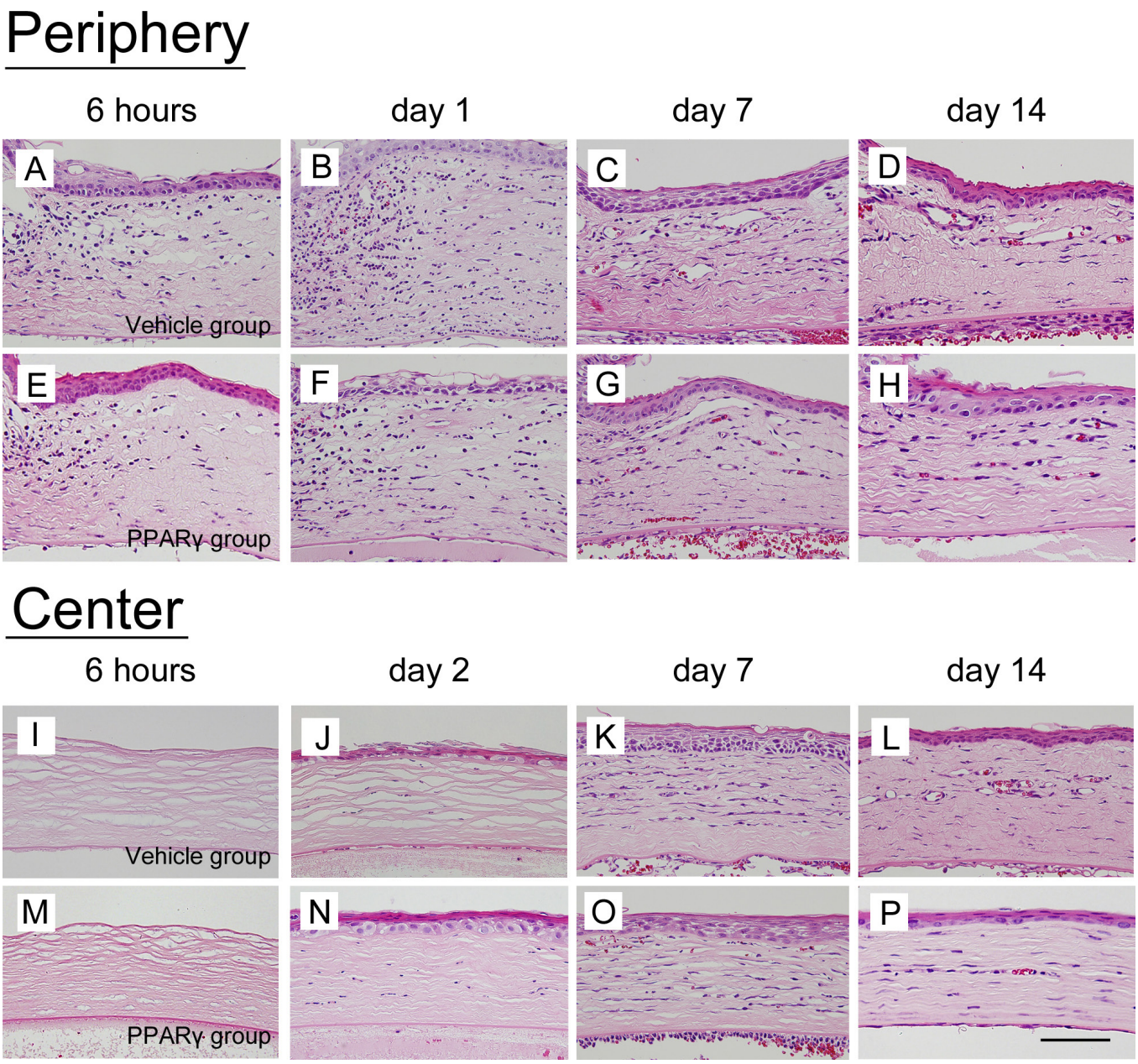

Figure 2. The corneal wound healing after alkali burn injury. The development of corneal wound healing after alkali injury in the vehicle (**A**–**D**: peripheral regions, **I**–**L**: central regions) and peroxisome proliferator-activated receptor γ (**E**–**H**: peripheral regions, **M**–**P**: central regions, scale bar: 100 μm) groups. After alkali injury in the vehicle and peroxisome proliferator-activated receptor gamma (PPARγ) groups, various inflammatory cells infiltrated from the corneal limbus into the corneal center by day 7. Between 6 h and day 1 after the injury, the inflammatory cells were prominent in the peripheral regions of the cornea, and were increased in the central regions of the cornea on day 7. After inflammatory cell infiltration, corneal neovascularization developed from the corneal limbus to the center by day 7 to day 14. The severity of the inflammatory cell infiltration and the degree of neovascularization in the cornea were decreased in the PPARγ group compared to the vehicle group.

cells/HPF, p=0.024) and macrophages (PPARγ group: 32.2±5.3 cells/HPF; vehicle group: 48.6±8.8 cells/HPF, p=0.049) peaked in the injured corneas in both groups (Figure 3E; Figure 4E). The ophthalmic solution of the PPARγ agonist reduced about 30% of the infiltrated neutrophils and macrophages in the corneas on day 1. In the PPARγ and vehicle groups, the number of neutrophils and macrophages was decreased in the corneal limbus, but increased in the

center of the cornea by day 7 (Figure 3C,D, Figure 4C,D). In the center regions of the corneas, the number of infiltrating neutrophils and macrophages peaked on day 7 with a second small peak of these cells in the entire cornea (neutrophils: 4.7±1.3 cells/HPF in the PPARγ group, 18.3±5.8 cells/HPF in the vehicle group, p=0.009; macrophages: 11.9±1.8 cells/HPF in the PPARγ group, 28.4±4.3 cells/HPF in the vehicle group, p=0.0005; Figure 3E, Figure 4E), but they were less prominent in the PPARγ group than in the vehicle group. The degree of infiltration of neutrophils and macrophages in the entire cornea was suppressed by PPARγ during the corneal inflammation and wound healing after alkali injury. In addition, in the PPARγ group, ED2-positive cells (M2 macrophages) were more prominent than in the vehicle group during corneal inflammation (Figure 5A–E). In the PPARγ group, the percentage of ED2-positive M2 macrophages in the total ED1-positive macrophage population was also increased compared to that in the vehicle group (Figure 5F). In the infiltrating macrophages, double immunohistochemical staining of ED2 and ED3 showed that ED3-positive activated macrophages were more prominent in the vehicle group, while ED2-positive M2 macrophages were increased in the PPARγ group (Figure 5G–L). These results indicated that the ophthalmic solution of the PPARγ agonist prevented the infiltration of neutrophils and macrophages in the rat alkali burn model. In addition, the ophthalmic solution of the PPARγ agonist increased the number of M2 macrophages in the inflamed cornea.

Neovascularization in alkali-burned corneas: In the PPARγ and vehicle groups, a few TM-positive capillaries appeared in the corneal limbus on day 1 or 2, indicating the presence of neovascularization. Then, neovascularization developed from the corneal limbus to the center of the cornea by day 7 (Figure 6A,B). On day 14, neovascularization was observed in the center of the cornea with narrowing capillary lumens in the PPARγ and vehicle groups (Figure 6C,D). In the macroscopic photographs, the central opacity and neovascularization of the cornea were less severe in the PPARγ group than in the vehicle group on day 14 (Figure 6E,F). The number of TM-positive capillary lumens in the entire cornea was significantly lower in the PPARγ group than in the vehicle group on days 4 and 7 (Figure 6G). In the entire cornea, 4.6±0.7 capillaries/HPF was noted on day 7 in the PPARγ group, and 8.5±0.8 capillaries/HPF was observed in the vehicle group (Figure 6G). The ophthalmic solution of the PPARγ agonist reduced more than 40% of the capillary lumens in the cornea on day 7. In addition, the number of capillary lumens in the entire cornea on day 14 was not significantly different for the PPARγ and vehicle groups (Figure 6G). However, in the center of the cornea, the number of capillary lumens was significantly lower (p=0.016) in the PPARγ group (5.6±0.6 capillary lumens/HPF) than in the vehicle group (8.3±0.8 capillary lumens/HPF).

Fibrotic reactions in alkali-burned corneas: In the normal cornea, the stromal collagen was composed primarily of type I collagen, with no or minimal deposition of type III collagen, and there was no accumulation of α-SMA-positive myofibroblasts (Figure 7A–C). On day 14, type I collagen was present in the alkali-burned corneas in the PPARγ and vehicle groups, similar to the normal cornea (Figure 7D,G). In the vehicle group, the deposition of type III collagen and accumulation of α-SMA-positive myofibroblasts was noted in the injured and inflammatory regions of the cornea (Figure 7E,F). However, the deposition of type III collagen and accumulation of α-SMA-positive myofibroblasts were obviously lower in the PPARγ group on day 14 (Figure 7H,I). The computer-assisted color image analysis indicated that the percentage of the positive pixel intensity of type III collagen in 200X corneal regions on day 14 were 0.5±0.1% in normal, 5.0±0.5% in the PPARγ group, and 15.2±2.7% in the vehicle group. The percentage of the α-SMA-positive cells in the corneal regions on day 14 was 0.1±0.05% in normal, 2.9±0.6% in the PPARγ group, and 6.7±0.9% in the vehicle group. The ophthalmic solution of the PPARγ agonist reduced the deposition of type III collagen (p=0.004) and the accumulation of α-SMA-positive myofibroblasts (p=0.005) in the cornea significantly on day 14.

Effects of the ophthalmic solution on the messenger ribonucleic acid expression levels after alkali burn injury: A real-time RT–PCR analysis was performed to assess the expression of genes associated with proinflammatory cytokines (IL-1β, IL-6, and TNF-α), chemotactic chemokines (IL-8 and MCP-1), the fibrotic reaction (TGF-β), and neovascularization (VEGF-A). In the alkali-burned corneas, the levels of the proinflammatory cytokines, such as IL-1β, IL-6, and TNF-α, were increased at 6 h and/or on day 1 during the development of corneal inflammation in the PPARγ and vehicle groups (Figure 8A–C). However, the increases in these molecules were suppressed by treatment with the ophthalmic solution of the PPARγ agonist at both time points. Thereafter, the mRNA levels of IL-1β, IL-6, and TNF-α gradually decreased by day 14. The expression levels of the chemotactic chemokines, IL-8 (neutrophil chemotactic factor) and MCP-1 (monocyte chemotactic chemokine), were also increased in the injured corneas after alkali exposure from 6 h in the PPARγ and vehicle groups. The peak levels for IL-8 and MCP-1 were noted on day 1 in the vehicle group and day 2 in the PPARγ group, but these levels were suppressed by treatment with the ophthalmic solution of the PPARγ agonist (Figure 8D,E).

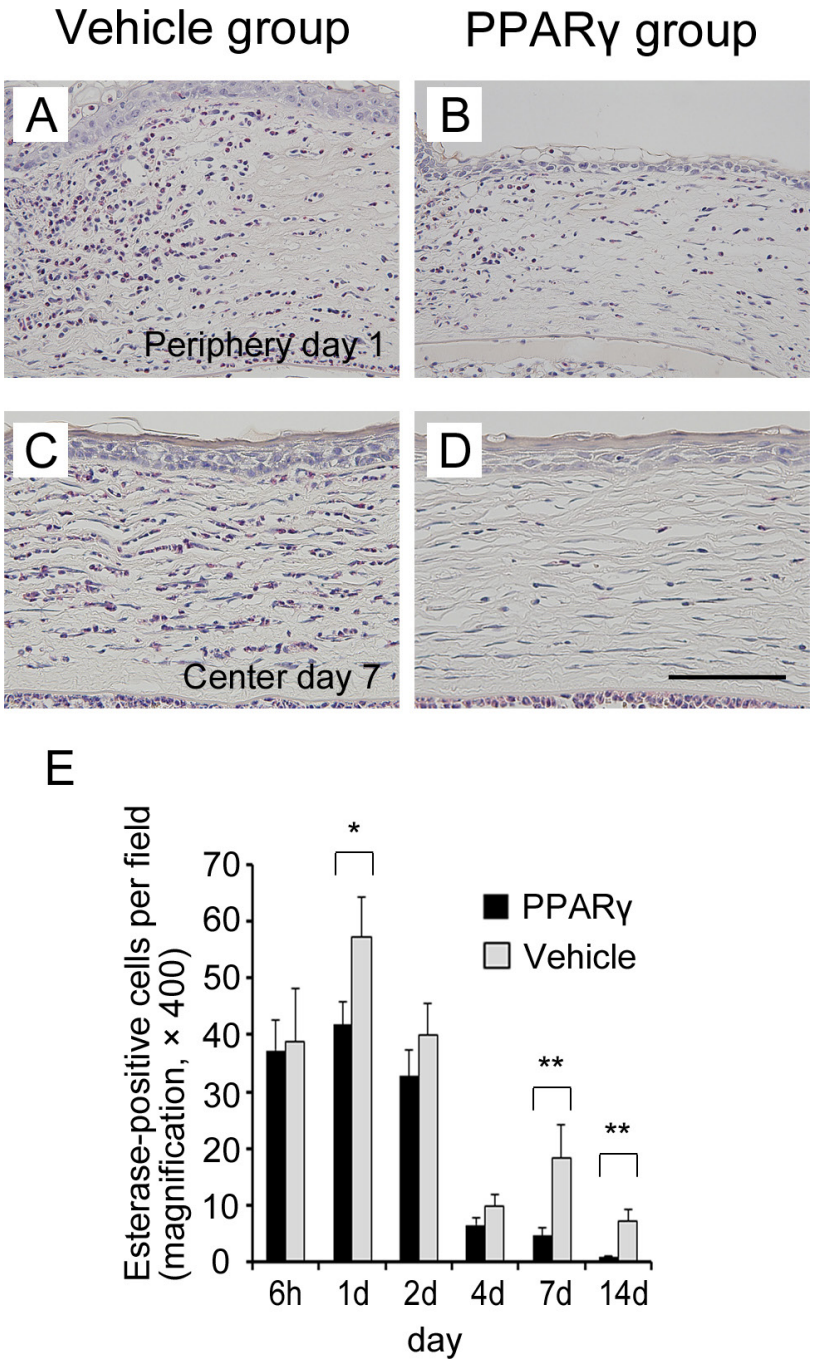

Figure 3. The infiltration of neutrophils in the alkali-burned cornea. Representative photomicrographs of infiltrating neutrophils in the vehicle (**A**, **C**) and peroxisome proliferator-activated receptor gamma (PPARγ) (**B**, **D**) groups on day 1 (**A**, **B**) and day 7 (**C**, **D**) after alkali injury (**A**–**D**: naphthol AS-D chloroacetate esterase stain, scale bar: 100 μm) showed that, in the vehicle and PPARγ groups, the neutrophil infiltration was prominent on day 1 in the peripheral regions of the cornea and on day 7 in the central regions of the cornea. The degree of neutrophil infiltration was less severe in the PPARγ group than in the vehicle group. **E**: The number of naphthol AS-D chloroacetate esterase-positive neutrophils per 400X high-power fields in the cornea showed that the infiltration of neutrophils in the cornea was significantly inhibited in the PPARγ group compared to the vehicle group on days 1, 7, and 14 in the alkali-burned cornea. The results are presented as the means±standard errors. *p<0.05, **p<0.01, compared with the vehicle group.

The mRNA levels of IL-8 and MCP-1 gradually decreased by day 14. The level of TGF-β1, which contributes to pathological fibrosis through the accumulation of myofibroblasts, increased and peaked at 6 h after the injury in the

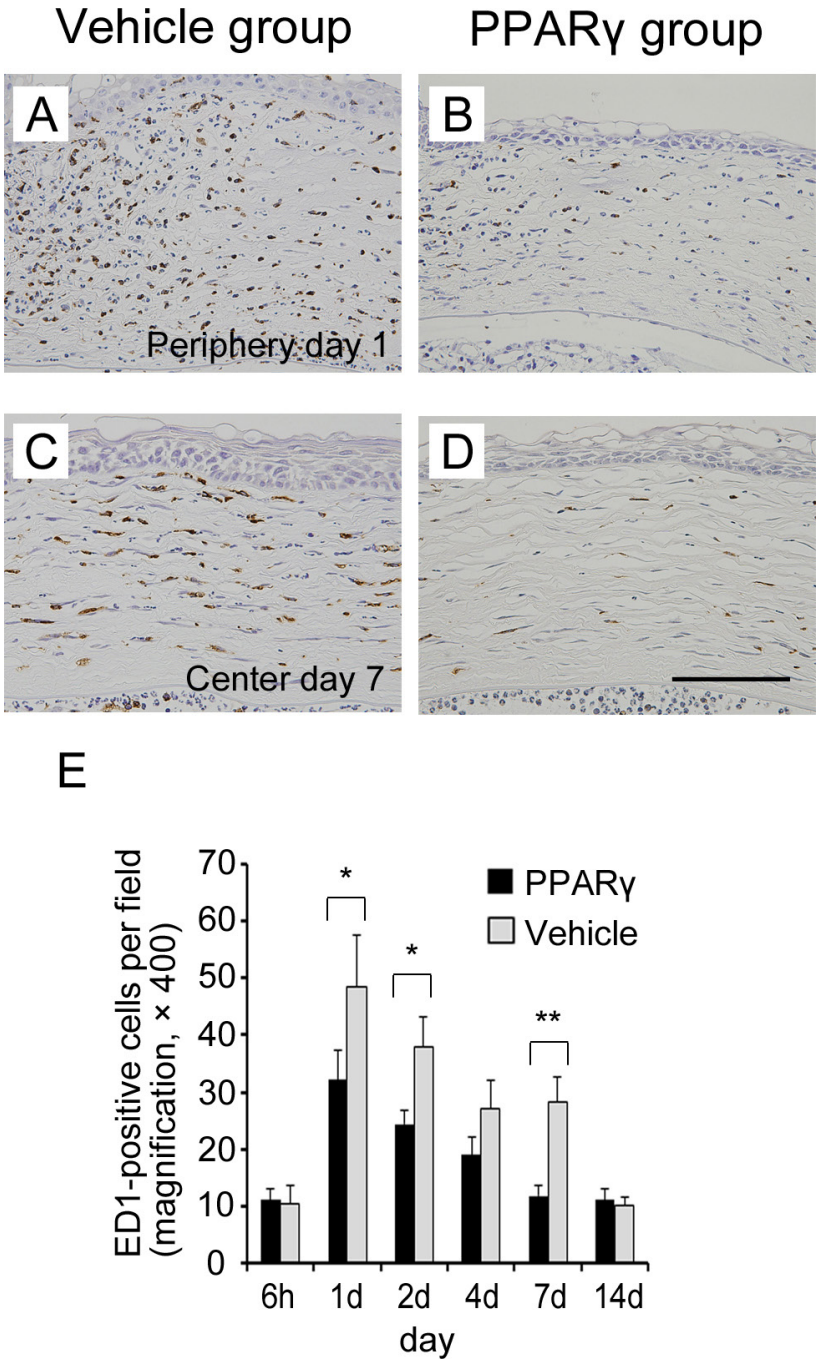

Figure 4. The infiltration of ED1-positive macrophages in alkali-burned corneas. Representative photomicrographs of infiltrating macrophages in the vehicle (**A**, **C**) and peroxisome proliferator-activated receptor gamma (PPARγ) (**B**, **D**) groups on day 1 (**A**, **B**) and day 7 (**C**, **D**) after alkali injury (**A**–**D**: ED1 stain, scale bar: 100 μm) showed that, in the vehicle and PPARγ groups, the macrophage infiltration was prominent on day 1 in the peripheral regions of the cornea and on day 7 in the central regions of the cornea. The degree of macrophage infiltration was less severe in the PPARγ group than in the vehicle group on day 1 and day 7. **E**: The number of ED1-positive macrophages per 400X high-power fields in the cornea showed that the macrophage infiltration in the cornea was significantly inhibited in the PPARγ group compared to the vehicle group on days 1, 2, and 7 in the alkali-burned cornea. The results are presented as the means±standard errors. *p<0.05, **p<0.01, compared with the vehicle group.

PPARγ and the vehicle groups (Figure 8F). The VEGF-A level also increased and peaked at 6 h after injury in both groups (Figure 8G). However, the increases in the mRNA levels of TGF-β1 and VEGF-A at 6 h were suppressed by the treatment

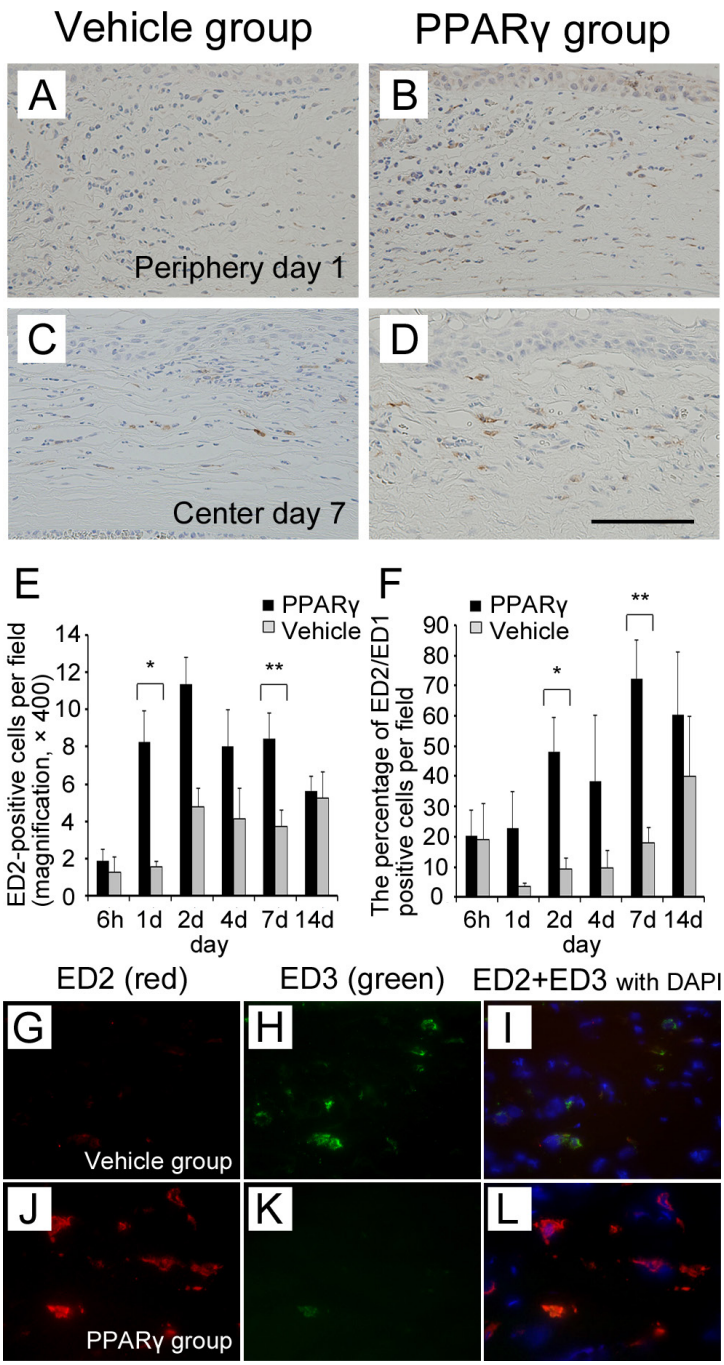

Figure 5. The infiltration of M2 macrophages in the alkali-burned cornea. Representative photomicrographs of infiltrating M2 macrophages in the vehicle (**A**, **C**) and peroxisome proliferator-activated receptor gamma (PPARγ) (**B**, **D**) groups on day 1 (**A**, **B**) and day 7 (**C**, **D**) after alkali injury (**A**–**D**: ED2 stain, scale bar: 100 μm) showed that, in the vehicle and PPARγ groups, the infiltration of ED2-positive M2 macrophages was prominent on day 1 in the peripheral regions of the cornea and on day 7 in the central regions of the cornea. The degree of M2 macrophage infiltration was more prominent in the PPARγ group than in the vehicle group. **E**: The number of ED2-positive M2 macrophages per 400X high-power fields in the cornea showed that the infiltration of M2 macrophages in the cornea was significantly increased in the PPARγ group compared to the vehicle group. **F**: The percentage of ED2-positive M2 macrophages in the total ED1-positive macrophages in the cornea showed that the percentage of M2 macrophages in the total macrophage population was increased more in the PPARγ group compared to the vehicle group. The results are presented as the means±standard errors. *p<0.05, **p<0.01, compared with the vehicle group. In the double immunofluorescence studies with ED2 (red; M2 marker; **G**, **J**) and ED3 (green; activated macrophage marker; **H**, **K**) in the vehicle and PPARγ groups on day 7, the ED2-positive M2 macrophages were more prominent than the ED3-positive activated macrophages in the PPARγ group (**J**–**L**, 800X), although the ED3-positive cells were more prominent than the ED2-positive cells in the vehicle group (**G**–**I**, 800X).

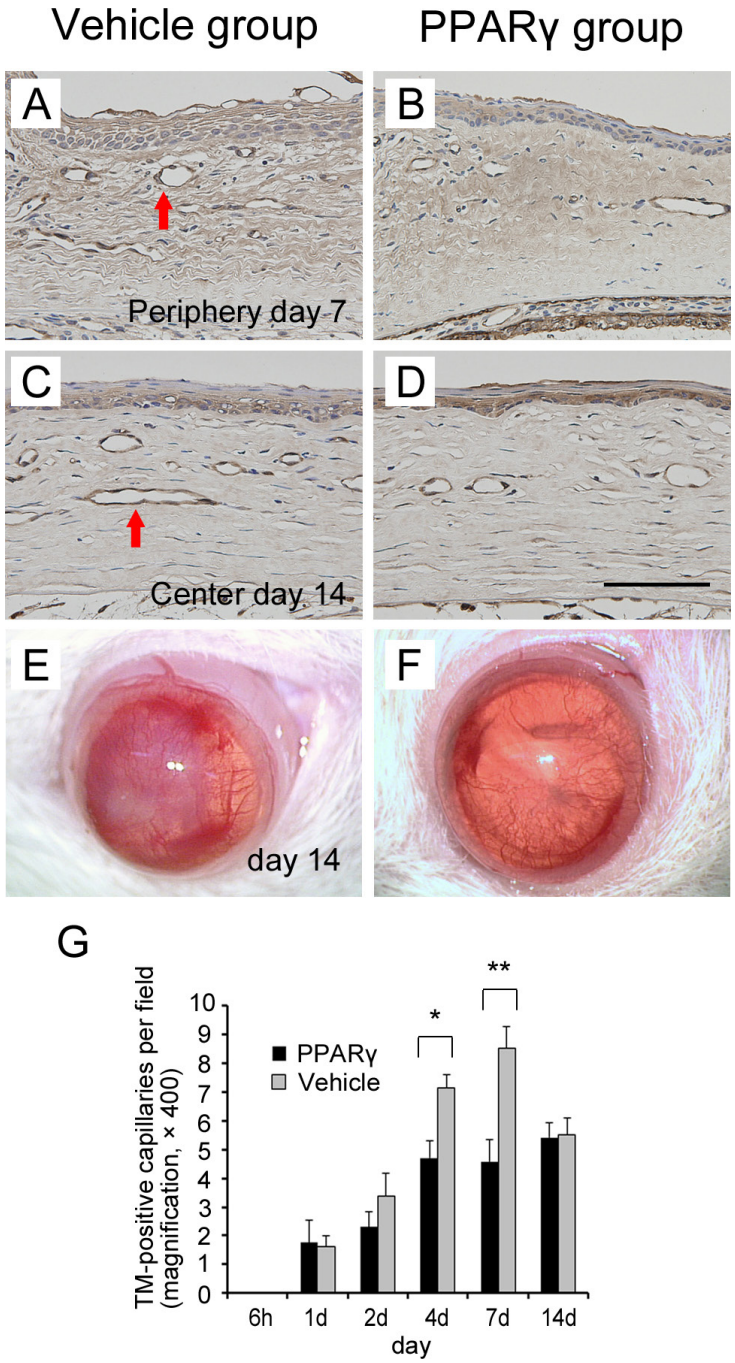

Figure 6. The central opacity and neovascularization of the cornea after alkali burn injury. The presence of thrombomodulin-positive capillaries (neovascularization) and photographs of the anterior segment in the alkali-burned cornea. Representative photomicrographs of neovascularization (arrow) in the vehicle (**A**, **C**) and peroxisome proliferator-activated receptor gamma (PPARγ) (**B**, **D**) groups on day 7 (**A**, **B**) and day 14 (**C**, **D**) after alkali injury (**A**–**D**: thrombomodulin [TM] stain, scale bar: 100 μm) showed that, in the vehicle and PPARγ groups, neovascularization was prominent in the peripheral regions of the cornea on day 7 and in the central regions of the cornea on day 14. Macroscopically, the central opacity and neovascularization of the cornea were less prominent in the PPARγ group (**F**) than in the vehicle group (**E**) on day 14. The degree of neovascularization was less prominent in the PPARγ group than in the vehicle group. **G**: The number of TM-positive capillary lumens per 400X high-power fields in the cornea showed that the neovascularization in the cornea was significantly inhibited in the PPARγ group compared to the vehicle group on days 4 and 7 in the alkali-burned cornea. The results are presented as the means±standard errors. *p<0.05, **p<0.01, compared with the vehicle group.

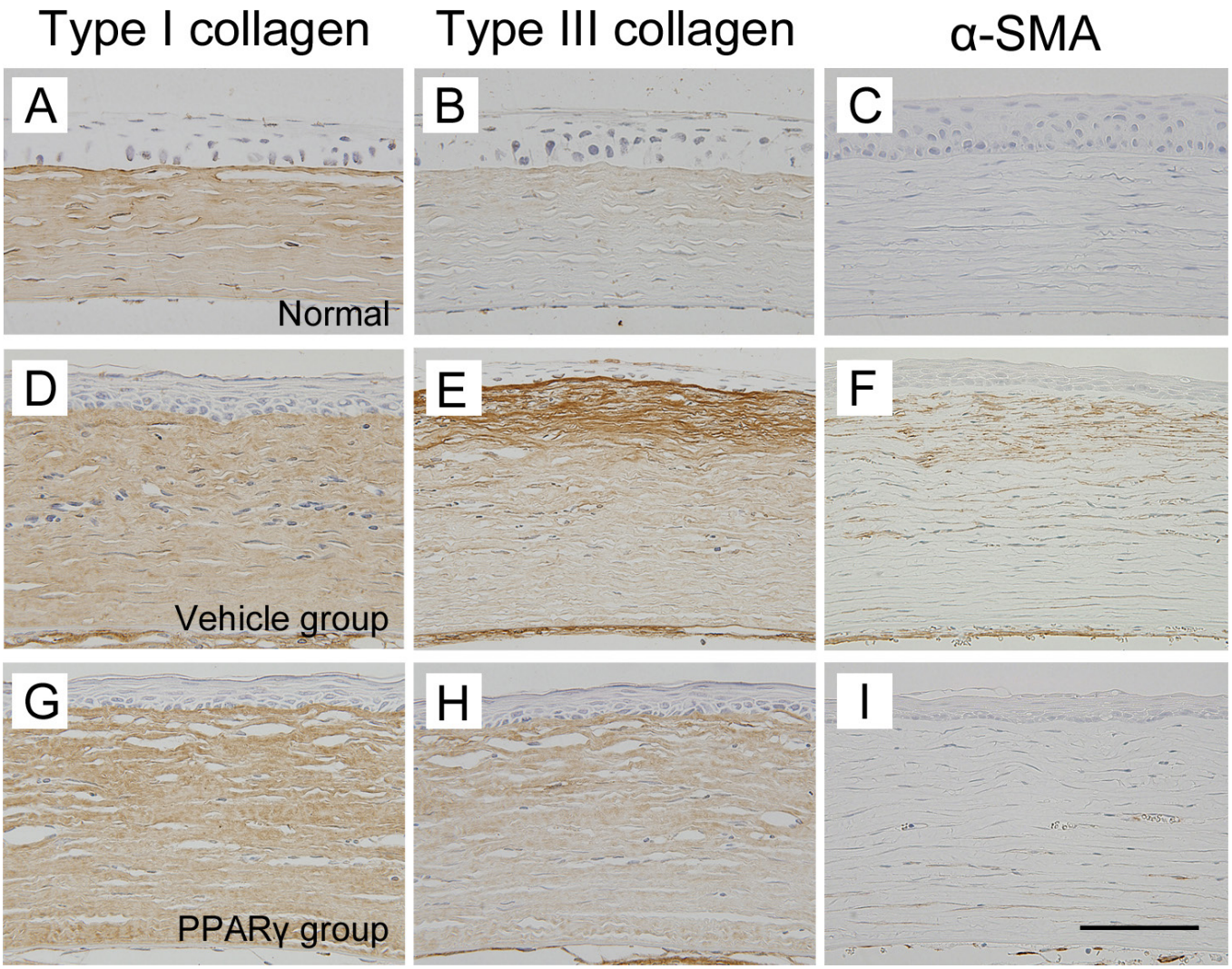

Figure 7. The deposition of type III collagen and accumulation of myofibroblasts in the cornea after alkali injury. The expression of type I (**A**, **D**, **G**) and III (**B**, **E**, **H**) collagen and α-smooth muscle actin (α-SMA, **C**, **F**, **I**) in the corneas in normal (**A**–**C**), vehicle-treated (**D**–**F**), and peroxisome proliferator-activated receptor gamma-treated (**G**–**I**) corneas (**A**, **D**, **G**: type I collagen stain; **B**, **E**, **H**: type III collagen stain; **C**, **F**, **I**: α-SMA stain, scale bar: 100 μm) on day 14. Type I collagen was the main collagen expressed in the cornea, and the deposition of type III collagen and accumulation of α-SMA-positive myofibroblasts was noted in the injured cornea, but was deposited to a lesser degree in the peroxisome proliferator-activated receptor gamma (PPARγ) group than in the vehicle group.

with the ophthalmic solution of the PPARγ agonist. Then, the mRNA levels gradually decreased by day 14. These results indicated that the PPARγ agonist-containing ophthalmic solution inhibited the functions of several molecules associated with proinflammatory, profibrotic, and neovascular reactions in the early phase after alkali injury.

DISCUSSION

The present study clarified that the ophthalmic solution of the PPARγ agonist can mediate anti-inflammatory, antifibrotic, and antineovascular effects in the cornea after an alkali burn injury. We considered that the ophthalmic solution was the most useful and clinical applicable method for corneal treatment, although we were initially concerned that the ophthalmic solution might be washed out by blinking. However, we confirmed that the ophthalmic solution of the PPARγ agonist had beneficial effects on corneal inflammation and wound healing. We therefore concluded that the ophthalmic solution of the PPARγ agonist may represent a new strategy for treating corneal inflammation and wound healing after corneal injury.

During the normal healing process in the alkali-burned cornea, the aqueous humor pH in the anterior chamber increases dramatically within 1 min due to the lysis of

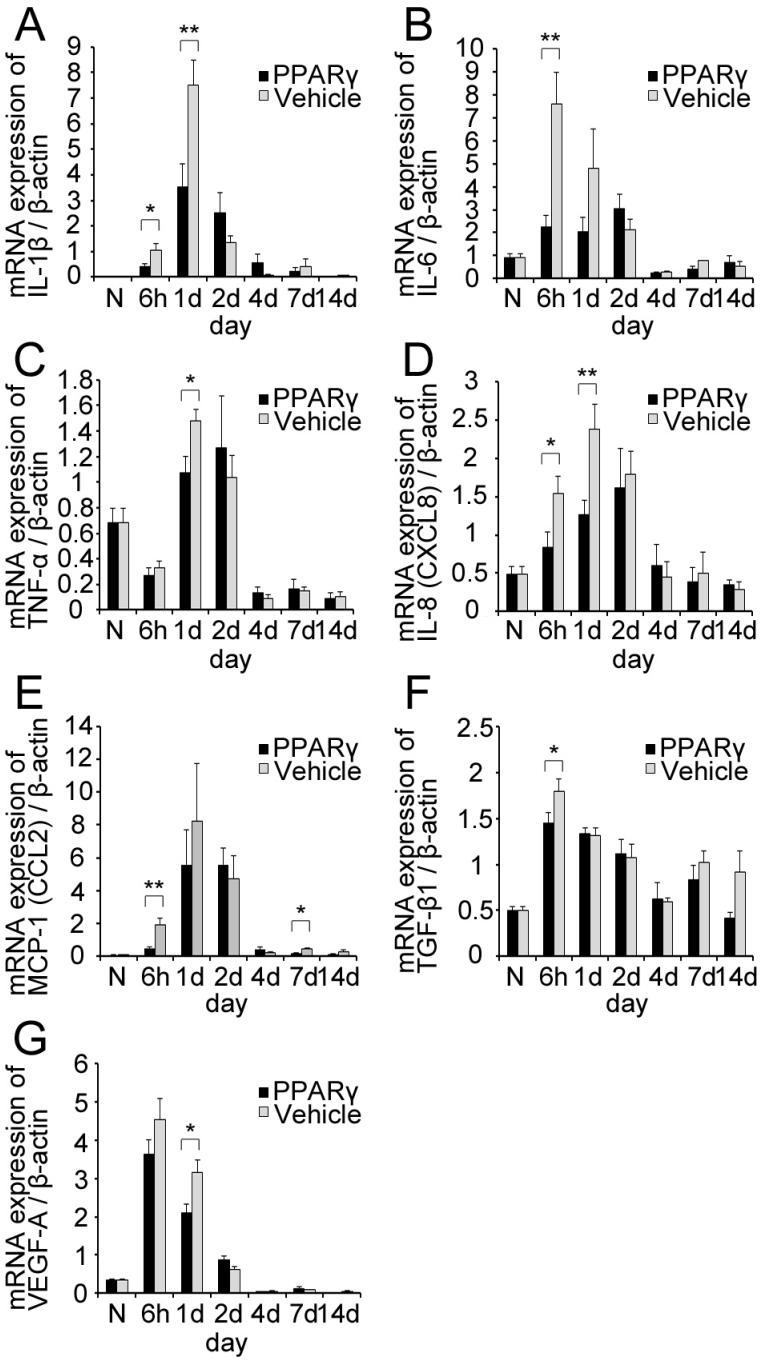

Figure 8. The expression of pro-inflammatory cytokines and chemokines in the cornea after alkali burn injury. Quantification of the messenger ribonucleic acid expression levels of (**A**) interleukin-1β, (**B**) interleukin-6, (**C**) tumor necrosis factor-α, (**D**) interleukin-8 (CXCL8), (**E**) monocyte chemoattractant protein-1, (**F**) transforming growth factor-β1, and (**G**) vascular endothelial growth factor-A. The messenger ribonucleic acid (mRNA) expression levels were measured with real-time reverse transcription–polymerase chain reaction (RT–PCR), and were normalized to the level of β-actin. A significant difference was observed between the vehicle and peroxisome proliferator-activated receptor gamma (PPARγ) groups at 6 h (**A**, **B**, **D**–**F**) and on day 1 (**A**, **C**, **D**, **G**) after injury. The "Normal" (N) in **A** to **G** indicates the mRNA values from uninjured normal corneas. The results are presented as the means±standard errors. *p<0.05, **p<0.01, compared with the vehicle group.

corneal cells, the blood-aqueous barrier is compromised, and necrotic debris is released into the aqueous humor [24]. Within 12–24 h, neutrophils and macrophages infiltrate into the peripheral cornea resulting from an outpouring of blood

elements from the injured vessels and necrotic tissue. In cases of severe alkali injury, a second wave of inflammatory cell infiltration begins at approximately 7 days after the injury [25]. The neutrophil infiltration into the cornea in the first wave may be critical for the recruitment in the second wave [26]. Thus, treatment of the first wave infiltration is effective for preventing the second wave and reducing the incidence of corneal ulceration in experimental alkali injuries [27].

In the present study, the corneal alkali injury and inflammation progressed similarly to those in the previous studies in the vehicle group. Infiltrating neutrophils increased first, and then the infiltrating macrophages increased soon after. In the peripheral cornea, the infiltrating neutrophils and macrophages peaked on the first day, and then increased in the center of the cornea on day 7. In the entire cornea, the first big wave of infiltrating neutrophils and macrophages was evident on day 1, and a second small wave was noted on day 7 in the vehicle group (Figure 3E, Figure 4E). In the PPARγ group, the infiltration of neutrophils and macrophages was less severe than that in the vehicle group in the first wave on day 1. Furthermore, the ophthalmic solution of the PPARγ agonist inhibited the infiltration of inflammatory cells not only in the first wave but also in the second smaller wave. The infiltration of neutrophils and macrophages on day 7 was significantly suppressed in the PPARγ group.

The cornea is an avascular tissue and must remain transparent to refract light properly. The light scattering by fibers results in an opaque cornea [28]. During the development and repair following stromal alkali injury, activated keratinocytes differentiate into corneal fibroblasts and myofibroblasts, and synthesize a higher proportion of collagen types III and V, while uninjured stromal collagen is predominantly type I [29]. The progression of neovascularization in the cornea mediates the irregular arrangement of collagen and exacerbates corneal scarring. In the present study, in the alkali-burned corneas on day 14, we confirmed the deposition of type III collagen and the accumulation of α-SMA-positive myofibroblasts, while the level of type I collagen was similar to that in the normal cornea. Treatment with a PPARγ ligand potently inhibited TGF-β-induced myofibroblast differentiation from corneal fibroblasts [30-32], and a PPARγ agonist inhibited the differentiation and expression of α-SMA in TGF-β1-activated fibroblasts, which was accompanied by a decrease in their production of collagen [33]. In accordance with these previous results, in the present study, the deposition of type III collagen and the accumulation of α-SMA-positive myofibroblasts were decreased significantly by the treatment with the ophthalmic solution of the PPARγ agonist. In addition, on day 14, the transparency of the central cornea was maintained more in the PPARγ group than in the vehicle group in macroscopic photographs. The ophthalmic solution of the PPARγ agonist led to less scarring of the central cornea, accompanied by reduced neovascularization, decreased type III collagen deposition, and suppressed myofibroblast accumulation.

In the field of macrophage-associated inflammation, recent studies have focused on the heterogeneity of macrophage activation and, in particular, on the ability of macrophages to amplify or curtail inflammation [34]. In response to the environmental milieu, macrophage changes can give rise to different populations of cells with distinct functions that are categorized as either classically activated (M1) or alternatively activated (M2) [35]. M1 macrophages are tissue injury–type macrophages involved mainly in the development of inflammation [36]. M1 macrophages are potent effector cells that kill microorganisms and produce proinflammatory cytokines such as IL-1β, IL-6, and TNF-α. In contrast, M2 macrophages have immunoregulatory and immunosuppressive functions. M2 macrophages dampen inflammation by producing anti-inflammatory factors, and influence tissue remodeling and repair [37]. Thus, in addition to the number of infiltrating macrophages, the macrophage phenotype is important for determining the outcome of inflammation. From this standpoint, PPARγ plays a significant role, because the activation of PPARγ polarizes the circulating blood monocytes to become M2 macrophages [38].

In the present study, the ophthalmic solution of a PPARγ agonist decreased the total number of infiltrating macrophages. In addition, the total number of M2 macrophages and the percentage of M2 macrophages compared with the total number of macrophages were increased by treatment with the ophthalmic solution of the PPARγ agonist. These results suggest that the ophthalmic solution of the PPARγ agonist promoted monocyte differentiation to M2 macrophages. M2 macrophages might have exerted immunoregulatory functions in corneal inflammation in the PPARγ group.

In the alkali-burned cornea, various cells, including epithelial, stromal, and inflammatory cells, are involved in the injury, repair, and wound healing processes, accompanied by the production of numerous cytokines. The wound healing reaction is orchestrated by various signals derived from endogenous soluble factors. IL-1β, IL-6, and TNF-α are all expressed in alkali-burned corneas, and IL-6, in particular, is strongly induced in the early stages after alkali burn injury in mice [39]. TGF-β is one of the most critical growth factors, and regulates the cellular responses involved in the process of wound healing and tissue inflammation [40]. MCP-1 and VEGF have been detected in post-alkali-burned corneas in mice [41]. In the present study, the expression of these genes

was reduced by treatment with an ophthalmic solution of a PPARγ agonist from the early phase after alkali injury. The differences in the expression levels of these genes between the PPARγ and vehicle groups may have been involved in the histological differences in the corneal inflammation and wound healing observed between the groups. These results suggest that the ophthalmic solution of the PPARγ agonist inhibited corneal inflammation at least partly by decreasing the expression of IL-1β, IL-6, TNF-α, IL-8, and MCP-1. In addition, the decreased deposition of type III collagen, inhibited accumulation of α-SMA-positive myofibroblasts, and suppressed neovascularization may be associated with the decrease in TGF-β1 and VEGF-A expression.

Tissue injury results in the activation of several transcription factors, including nuclear factor κB, signal transducer and activator of transcription, and activated protein-1, which results in the upregulation of the genes for several primarily proinflammatory cytokines and chemokines, all of which act in concert to orchestrate an inflammatory response [1]. When the initial and the early inflammatory response is excessive, this may further aggravate the tissue injury. The activation of PPARγ inhibits the activation of the transcription factors nuclear factor κB, signal transducer and activator of transcription, and activated protein-1 [1,5,8,34]. This subsequently attenuates the formation of cytokines (such as IL-1β, IL-6, and TNF-α) and chemokines (such as IL-8 and MCP-1) and, therefore, reduces excessive inflammation and tissue injury. Indeed, in the present study, reduction of these cytokines and chemokines was evident in the early period after the alkali burn injury. This mechanism associated with transcription factors may be one of the most important mechanisms of anti-inflammation, antifibrotic reaction, and antineovascularization in the present study. Further investigations are necessary concerning the mechanisms of the beneficial effects of ophthalmic solution of the PPARγ agonist on the corneal inflammation and wound healing after injury.

Conclusion: We compounded an ophthalmic solution of a PPARγ agonist using pioglitazone hydrochloride, and instilled it on the corneas to treat alkali burn injuries in rats. The ophthalmic solution of the PPARγ agonist inhibited inflammation, decreased the fibrotic reaction, and prevented neovascularization associated with the burn injury. The anti-inflammatory, antifibrotic, and antineovascularization effects exerted by the ophthalmic solution of the PPARγ agonist were accompanied by a decrease in the mRNA expression of proinflammatory, profibrotic, and neovascularization factors in the early phase of the response to the alkali burn injury. The ophthalmic solution of the PPARγ agonist had beneficial effects on corneal inflammation and wound healing of the cornea after injury. We therefore concluded that the ophthalmic solution of the PPARγ agonist may represent a new strategy for treating corneal inflammation and would improve healing after corneal injury.

ACKNOWLEDGMENTS

We are grateful to Dr. Mika Terasaki, Analytic Human Pathology, Nippon Medical School, for the special advice and critical review of the manuscript. We express special thanks to Mr. Takashi Arai, Ms. Mitue Kataoka, Kyoko Wakamatu, Arimi Ishikawa and Naomi Kuwahara for their expert technical assistance. We are also grateful to Dr. Yoichi Kawashima for his useful suggestions about compounding the ophthalmic solution for the present study. This study was supported by Nippon Medical School Grant-in-aid for Medical Research, Tokyo, Japan. This funding organization had no role in the design or conduct of this research.

REFERENCES

1. Abdelrahman M, Sivarajah A, Thiemermann C. Beneficial effects of PPAR-gamma ligands in ischemia-reperfusion injury, inflammation and shock. Cardiovasc Res 2005; 65:772-81. [PMID: 15721857].
2. Evans RM. The steroid and thyroid hormone receptor superfamily. Science 1988; 240:889-95. [PMID: 3283939].
3. Tyagi S, Gupta P, Saini AS, Kaushal C, Sharma S. The peroxisome proliferator-activated receptor: A family of nuclear receptors role in various diseases. J Adv Pharm Technol Res 2011; 2:236-40. [PMID: 22247890].
4. Széles L, Töröcsik D, Nagy L. PPARgamma in immunity and inflammation: cell types and diseases. Biochim Biophys Acta 2007; 1771:1014-30. [PMID: 17418635].
5. Schmidt MV, Brüne B, von Knethen A. The nuclear hormone receptor PPARγ as a therapeutic target in major diseases. ScientificWorldJournal 2010; 10:2181-97. [PMID: 21057731].
6. Ricote M, Li AC, Willson TM, Kelly CJ, Glass CK. The peroxisome proliferator-activated receptor-gamma is a negative regulator of macrophage activation. Nature 1998; 391:79-82. [PMID: 9422508].
7. Jiang C, Ting AT, Seed B. PPAR-gamma agonists inhibit production of monocyte inflammatory cytokines. Nature 1998; 391:82-6. [PMID: 9422509].
8. von Knethen A, Brüne B. PPARgamma–an important regulator of monocyte/macrophage function. Arch Immunol Ther Exp (Warsz) 2003; 51:219-26. [PMID: 12956430].
9. Aljada A, O'Connor L, Fu YY, Mousa SA. PPAR gamma ligands, rosiglitazone and pioglitazone, inhibit bFGF- and VEGF-mediated angiogenesis. Angiogenesis 2008; 11:361-7. [PMID: 18810647].
10. Hatanaka H, Koizumi N, Okumura N, Kay EP, Mizuhara E, Hamuro J, Kinoshita S. Epithelial-mesenchymal

transition-like phenotypic changes of retinal pigment epithelium induced by TGF-β are prevented by PPAR-γ agonists. Invest Ophthalmol Vis Sci 2012; 53:6955-63. [PMID: 22956604].

11. Taguchi K, Okada A, Yasui T, Kobayashi T, Ando R, Tozawa K, Kohri K. Pioglitazone, a peroxisome proliferator activated receptor γ agonist, decreases renal crystal deposition, oxidative stress and inflammation in hyperoxaluric rats. J Urol 2012; 188:1002-11. [PMID: 22819112].
12. Yu Y, Zhang ZH, Wei SG, Weiss RM, Felder RB. Peroxisome proliferator-activated receptor-γ regulates inflammation and renin-angiotensin system activity in the hypothalamic paraventricular nucleus and ameliorates peripheral manifestations of heart failure. Hypertension 2012; 59:477-84. [PMID: 22083161].
13. Reddy AT, Lakshmi SP, Kleinhenz JM, Sutliff RL, Hart CM, Reddy RC. Endothelial cell peroxisome proliferator-activated receptor γ reduces endotoxemic pulmonary inflammation and injury. J Immunol 2012; 189:5411-20. [PMID: 23105142].
14. Saika S, Yamanaka O, Okada Y, Miyamoto T, Kitano A, Flanders KC, Ohnishi Y, Nakajima Y, Kao WW, Ikeda K. Effect of overexpression of PPARgamma on the healing process of corneal alkali burn in mice. Am J Physiol Cell Physiol 2007; 293:C75-86. [PMID: 17625041].
15. Sarayba MA, Li L, Tungsiripat T, Liu NH, Sweet PM, Patel AJ, Osann KE, Chittiboyina A, Benson SC, Pershadsingh HA, Chuck RS. Inhibition of corneal neovascularization by a peroxisome proliferator-activated receptor-gamma ligand. Exp Eye Res 2005; 80:435-42. [PMID: 15721625].
16. Gao D, Ning N, Hao G, Niu X. Pioglitazone attenuates vascular fibrosis in spontaneously hypertensive rats. PPAR Res 2012; 2012:856426-[PMID: 22550475].
17. Wahli W, Michalik L. PPARs at the crossroads of lipid signaling and inflammation. Trends Endocrinol Metab 2012; 23:351-63. [PMID: 22704720].
18. Masuda Y, Shimizu A, Mori T, Ishiwata T, Kitamura H, Ohashi R, Ishizaki M, Asano G, Sugisaki Y, Yamanaka N. Vascular endothelial growth factor enhances glomerular capillary repair and accelerates resolution of experimentally induced glomerulonephritis. Am J Pathol 2001; 159:599-608. [PMID: 11485918].
19. Fujita E, Shimizu A, Masuda Y, Kuwahara N, Arai T, Nagasaka S, Aki K, Mii A, Natori Y, Iino Y, Katayama Y, Fukuda Y. Statin attenuates experimental anti-glomerular basement membrane glomerulonephritis together with the augmentation of alternatively activated macrophages. Am J Pathol 2010; 177:1143-54. [PMID: 20696778].
20. Ohashi R, Shimizu A, Masuda Y, Kitamura H, Ishizaki M, Sugisaki Y, Yamanaka N. Peritubular capillary regression during the progression of experimental obstructive nephropathy. J Am Soc Nephrol 2002; 13:1795-805. [PMID: 12089375].
21. Shimizu A, Masuda Y, Mori T, Kitamura H, Ishizaki M, Sugisaki Y, Fukuda Y. Vascular endothelial growth factor165 resolves glomerular inflammation and accelerates glomerular capillary repair in rat anti-glomerular basement membrane glomerulonephritis. J Am Soc Nephrol 2004; 15:2655-65. [PMID: 15466270].
22. Wakamatsu K, Ghazizadeh M, Ishizaki M, Fukuda Y, Yamanaka N. Optimizing collagen antigen unmasking in paraffin-embedded tissues. Histochem J 1997; 29:65-72. [PMID: 9088946].
23. Tanabe M, Shimizu A, Masuda Y, Kataoka M, Ishikawa A, Wakamatsu K, Mii A, Fujita E, Higo S, Kaneko T, Kawachi H, Fukuda Y. Development of lymphatic vasculature and morphological characterization in rat kidney. Clin Exp Nephrol 2012; 16:833-42. [PMID: 22581062].
24. Pfister RR, Pfister DR. Alkali injuries of the eye. In: Krachmer JH, mannis MJ, Holland EJ, editors. CORNEA. 2nd Edition ed2005. p. 1285–93.
25. Paterson CA, Williams RN, Parker AV. Characteristics of polymorphonuclear leukocyte infiltration into the alkali burned eye and the influence of sodium citrate. Exp Eye Res 1984; 39:701-8. [PMID: 6097468].
26. Wagoner MD. Chemical injuries of the eye: current concepts in pathophysiology and therapy. Surv Ophthalmol 1997; 41:275-313. [PMID: 9104767].
27. Pfister RR, Haddox JL, Lank KM. Citrate or ascorbate/citrate treatment of established corneal ulcers in the alkali-injured rabbit eye. Invest Ophthalmol Vis Sci 1988; 29:1110-5. [PMID: 3417403].
28. Maurice DM. The structure and transparency of the cornea. J Physiol 1957; 136:263-86. [PMID: 13429485].
29. Saika S, Ooshima A, Shima K, Tanaka S, Ohnishi Y. Collagen types in healing alkali-burned corneal stroma in rabbits. Jpn J Ophthalmol 1996; 40:303-9. [PMID: 8988419].
30. Kuriyan AE, Lehmann GM, Kulkarni AA, Woeller CF, Feldon SE, Hindman HB, Sime PJ, Huxlin KR, Phipps RP. Electrophilic PPARγ ligands inhibit corneal fibroblast to myofibroblast differentiation in vitro: a potentially novel therapy for corneal scarring. Exp Eye Res 2012; 94:136-45. [PMID: 22178289].
31. Pan H, Chen J, Xu J, Chen M, Ma R. Antifibrotic effect by activation of peroxisome proliferator-activated receptor-gamma in corneal fibroblasts. Mol Vis 2009; 15:2279-86. [PMID: 19936025].
32. Pan HW, Xu JT, Chen JS. Pioglitazone inhibits TGFβ induced keratocyte transformation to myofibroblast and extracellular matrix production. Mol Biol Rep 2011; 38:4501-8. [PMID: 21127991].
33. Lee HM, Kang HJ, Park HH, Hong SC, Kim JK, Cho JH. Effect of peroxisome proliferator-activated receptor gamma agonists on myofibroblast differentiation and collagen production in nasal polyp-derived fibroblasts. Ann Otol Rhinol Laryngol 2009; 118:721-7. [PMID: 19894400].
34. Gordon S, Taylor PR. Monocyte and macrophage heterogeneity. Nat Rev Immunol 2005; 5:953-64. [PMID: 16322748].

35. Ricardo SD, van Goor H, Eddy AA. Macrophage diversity in renal injury and repair. J Clin Invest 2008; 118:3522-30. [PMID: 18982158].

36. Mosser DM. The many faces of macrophage activation. J Leukoc Biol 2003; 73:209-12. [PMID: 12554797].

37. Bouhlel MA, Derudas B, Rigamonti E, Dièvart R, Brozek J, Haulon S, Zawadzki C, Jude B, Torpier G, Marx N, Staels B, Chinetti-Gbaguidi G. PPARgamma activation primes human monocytes into alternative M2 macrophages with anti-inflammatory properties. Cell Metab 2007; 6:137-43. [PMID: 17681149].

38. Charo IF. Macrophage polarization and insulin resistance: PPARgamma in control. Cell Metab 2007; 6:96-8. [PMID: 17681144].

39. Sotozono C, He J, Matsumoto Y, Kita M, Imanishi J, Kinoshita S. Cytokine expression in the alkali-burned cornea. Curr Eye Res 1997; 16:670-6. [PMID: 9222084].

40. Saika S. TGFbeta pathobiology in the eye. Lab Invest 2006; 86:106-15. [PMID: 16341020].

41. Saika S, Ikeda K, Yamanaka O, Miyamoto T, Ohnishi Y, Sato M, Muragaki Y, Ooshima A, Nakajima Y, Kao WW, Flanders KC, Roberts AB. Expression of Smad7 in mouse eyes accelerates healing of corneal tissue after exposure to alkali. Am J Pathol 2005; 166:1405-18. [PMID: 15855641].

Articles are provided courtesy of Emory University and the Zhongshan Ophthalmic Center, Sun Yat-sen University, P.R. China. The print version of this article was created on 1 November 2013. This reflects all typographical corrections and errata to the article through that date. Details of any changes may be found in the online version of the article.